RADINKA JOURNAL OF SCIENCE AND SYSTEMATIC LITERATURE REVIEW

ISSN 2988-5825

https://www.rjupublisher.com/ojs/index.php/RJSLR

Petrogenetic and Geothermobarometric Constraints on the Twin Panyam Volcanoes, Jos Plateau, North-Central Nigeria

Lekmang, ISAH C[a*], Achuenu IFEANYI[b], Lar, U. ALEXANDER[b]

[a]*Department of Geology, University of Jos Plateau State, Nigeria*
[b]*Department of Mining Engineering, University of Jos Plateau State, Nigeria*

*Corresponding author: achuenuifeanyi@gmail.com

Abstract

The Twin Panyam volcanoes of the Jos Plateau, north-central Nigeria, constitute one of the most prominent centers of Neogene–Quaternary alkaline volcanism within the Benue–Cameroon volcanic Province. This study integrates petrographic, whole-rock geochemical, and mineral thermobarometric data to constrain the petrogenetic evolution and magmatic conditions of the Panyam volcanic system. Field observations and thin-section analyses reveal porphyritic to intergranular textures dominated by olivine, augite, labradorite, and Fe–Ti oxides, consistent with basaltic to trachybasaltic magma compositions. Whole-rock geochemistry classifies the lavas as alkaline basalts characterized by elevated total alkali contents (Na_2O + K_2O). Mineral-based geothermobarometric estimates yield crystallization temperatures of 800–1,000 °C and pressures of 6–9 kbar, indicating magma storage within upper-mantle to lower-crustal depths. These results suggest that the Twin Panyam volcanoes evolved through fractional crystallization of an alkaline basaltic magma derived from a mildly enriched lithospheric mantle source. Generally, the findings enhance current understanding of post-Miocene volcanic processes on the Jos Plateau and provide insights into its broader geodynamic connection with the Cameroon Volcanic Line.

Keywords: Alkaline basalts petrogenetic, geodynamic, geothermobarometric, petrographic, geochemical,

Acknowledgments: The authors would like to express their sincere gratitude to the local authorities and field guides in the Jos Plateau region for their invaluable assistance and logistical support during the field campaigns and sample collection. Special thanks are extended to the laboratory personnel and technical staff who facilitated the thin-section preparation, petrographic analyses, and whole-rock geochemical testing. We also acknowledge the institutional support provided by our respective research facilities and universities, which greatly contributed to the successful execution of this study.

For citation:
Isah C. L., Ifeanyi, A & Alexander, L. U. (2026). Petrogenetic and Geothermobarometric Constraints on the Twin Panyam Volcanoes, Jos Plateau, North-Central Nigeria. *Radinka Journal of Science and Systematic Literature Review, 4*(2), 920-934.

Introduction

The Jos Plateau, located in north-central Nigeria, is a high-relief dome structure characterized by massive Neogene–Quaternary volcanic activity. Evidence of this volcanism is clearly preserved in the form of volcanic cones, lava flows, and pyroclastic deposits distributed widely across the region (Benamrane et al., 2022; Tomasi et al., 2023). These hills and volcanic cones provide strong evidence of past eruptive episodes closely linked to mantle-derived magmatism. In terms of regional geology, the Nigerian landmass—covering an area of approximately 923,768 km²—is underlain by a nearly equal proportion of crystalline basement rocks and sedimentary rock sequences. Within this framework, volcanic rocks are predominantly found in the central and northeastern sectors. This volcanism represents the youngest magmatic event to intrude the Nigerian basement terrain. The occurrence of volcanic rocks in this region is not random but structurally controlled. These magmatic features exhibit alignments parallel to fracture zones trending north-northwest to south-southeast (NNW–SSE). This structural system is tectonically linked to the Benue Trough and the Cameroon Volcanic Line (Jimenez et al., 2025; Acosta-Nagle et al., 2025).

As part of the Cenozoic volcanic province of north-central Nigeria, the Jos Plateau forms a regional volcanic complex alongside the Biu, Kapsiki, and Longuda plateaus. Locally, the complex overlies the Precambrian Nigerian Basement Complex—dominated by granite, gneiss, and migmatite—and is bounded to the southeast by the Benue Trough. Volcanism on the Jos Plateau is generally alkaline in nature and occurred episodically from the Miocene through the Late Quaternary (Szakács & Kovacs, 2022; Cedric Bernard & Uriah Alexander, 2022). Lithologically, the volcanic sequence on the Jos Plateau is dominated by basalt, trachybasalt, phonolite, and pyroclastic material. One of the most prominent eruptive centers in the region is the Twin Panyam volcanic complex, located near Kerang. This volcanic center forms small cones aligned along a NNW–SSE fracture zone, indicating strong tectonic control over the spatial arrangement and magma ascent to the surface (Hategekimana et al., 2024; Principe et al., 2024; Udoinyang, 2025).

Field observations in the Twin Panyam area reveal well-preserved basaltic cones and associated lava flows overlying older fluvio-volcanic deposits. Petrographic and geochemical data indicate that both the "Older" and "Newer" , and Fe–Ti oxides (Heineke et al., 2016; Kang et al., 2025). On a regional geodynamic scale, the volcanic rocks of the Jos Plateau are associated with lithospheric extension and mantle upwelling linked to the activity of the Cameroon Volcanic Line (CVL) (Németh & Kósik, 2020; Verolino et al., 2022). This geodynamic association implies that the Panyam volcanic rocks originated from mildly enriched mantle melts. These magmas ascended through reactivated basement fractures, underwent limited crustal interaction (Issatayeva et al., 2025; Pompa-Mera et al., 2026), and solidified to form cones and flows of alkaline basalt. Although this region has been the subject of various prior petrographic and geochemical studies(Lima & Ottosen, 2021), quantitative constraints on magma formation conditions remain limited. In particular, comprehensive information regarding mineral equilibration temperatures and pressures for the Panyam volcanoes has not yet been established.

The lack of quantitative data on crystallization temperatures and pressures poses a major obstacle to precisely reconstructing magmatic evolution. Yet, a deep understanding of thermobarometric parameters is crucial for deciphering the magma evolution and mantle processes underlying volcanism in north-central Nigeria. To address this knowledge gap, this study employs an integrated approach combining geothermobarometry and geochemistry. This approach aims to: classify the basaltic rocks of the Twin Panyam volcanoes, (determine the temperature and pressure conditions during crystallization, and interpret their petrogenetic evolution within the broader framework of Jos Plateau volcanism.

Methodology

This section outlines the field, laboratory, and analytical procedures employed in this study, as well as the mathematical and geothermobarometric models adopted to interpret the mineralogical and geochemical characteristics of the Twin Panyam volcanic rocks. The workflow integrated petrographic examination, mineral chemistry, and geochemical analyses to establish the petrogenetic evolution and classification of the volcanic suite.

Laboratory Procedures

Petrographic Analysis

Six (6) representative rock samples were cut into standard thin sections and examined using a polarizing petrographic microscope under both plane- and cross-polarized light. This facilitated the identification of the primary and secondary mineral phases, textural relationships, and alteration features, following standard procedures outlined by (Rojas et al., 2026).

Lectron Microprobe Analysis (EMPA)

The six (6) representative samples which were examined using the polarizing petrographic microscope were further analyzed using a CAMECA SX-50 Electron Microprobe at the Electron Microprobe Laboratory, University of Minnesota, USA. The analyses targeted coexisting mineral phases (olivine, pyroxene, and plagioclase) under accelerating voltage of 15 kV, beam current of 11 nA, and counting time of 10 seconds. Analytical precision was better than ±2%. Structural formulae were computed from stoichiometric oxide proportions following Deer et al. (2019), and mineral end-members were determined for comparison with global basaltic suites (Scivetti & Teobaldi, 2023); (Neave et al., 2024).

Sample Preparation and Geochemical Analysis

The previously examined samples (6) for petrography were pulverized to <63 µm using a tungsten carbide mill at the Department of Geology, Ahmadu Bello University, Zaria. Approximately 2 g of each powdered sample was sealed in polythene bags and sent to Acme Analytical Laboratories Ltd., Vancouver, Canada, for major, trace, and rare earth element (REE) analyses. Major oxides were determined by X-Ray Fluorescence (XRF) after lithium metaborate fusion, while trace and rare earth elements were measured using Inductively Coupled Plasma Mass Spectrometry (ICP-MS). The analytical suite included major oxides (SiO_2, Al_2O_3, Fe_2O_3, MgO, MnO, CaO, Na_2O, K_2O, TiO_2, and P_2O_5), trace elements (Be, Cr, Ni, Co, V, Cu, Pb, Zn, Mo, W, Rb, Cs, Ba, Sr, Ga, Nb, Ta, Zr, Hf, Y, Th, and U), and REEs (La–Lu). Accuracy and precision were better than 0.01 wt% for major elements and ±0.1 ppm for trace and REEs, based on repeated runs of certified international rock standards.

Mathematical and Geothermobarometric Modelling

To further constrain crystallization conditions, empirical thermodynamic relationships between Bowen's Reaction Series and Goldschmidt's Element Partitioning Rules were expressed mathematically following the modified binomial expansion of (Martínez-Casado et al., 2019). The model assumes that the distribution of ions in a silicate melt (Z_0) is a function of the ratio of silicate radicals (z^-) to cations (x^+) under electrolytic equilibrium, where $n + p = \eta + p$, with η representing magma strength ($\mathfrak{M}$).

Anhydrous Melt ($\mathfrak{W}$)

An anhydrous melt refers to magma with negligible water content, silica undersaturation, and low viscosity, characteristic of mafic volcanic systems. The mineral series derived from this melt were computed using parametric expressions for olivine, pyroxene, and plagioclase solid solutions.

Mafic Olivine Series

$$[\mathrm{Mg} + \mathrm{iFe}]_2\ Si\ O_4\ = Mg_2\ Si\ O_4\ + i[Mg\ \mathrm{Fe}]Si\ O_4 + i[\mathrm{MgFe}]SiO_4\ + Fe_2\ Si\ O_4$$

According to Achuenu and others (2025), $Mg_{2-p}Fe_pSiO_4$ is an '<u>Olivine series'</u> formula that can be used to calculate all olivine minerals from the melt $\mathfrak{W}$, where p is an integer and ranges from 0 to 2 in olivine crystals. At p equals to zero, 100% Forsterite (Fo) crystallizes with chemical formula of Mg_2SiO_4 and at p equals to 2, Forsterite (fo) disappears and 100% of pure Fayalite (Fa) crystallizes with chemical formula of $Fe_2SiO_{4(s)}$. Therefore forsterite, Hyalosiderite, Hortornolite and fayalite are the primary olivine in the mafic olivine series. Intermediate compositions represent the Fo–Fa solid solution series (Forsterite–Fayalite),

Mafic Pyroxene Series

$$\sum_{n=\mathrm{r}}^{\mathrm{p}} \binom{n}{p} \quad [\beta + \alpha]_{n+p}\ Si_2\ O_6\ = Mg_2\ Si_2\ O_6\ \ + i[Mg\ \mathrm{Fe}]\ Si_2\ \ O_6 + i[\mathrm{MgFe}]Si_2\ O_6\ + Fe_2\ Si_2\ O_6$$

$Mg_{2-p}Fe_pSi_2O_6$ is a pyroxene series, where p ranges from 0 to 2 in pyroxene. At p equals to zero, 100% Enstatite (En) crystallizes with chemical formula of $Mg_2Si_2O_6$ and at p equals to 2, Enstatite disappears and 100% of pure Ferrosilite crystallizes with chemical formula of $Fe_2Si_2O_6$ Therefore Enstaite, Hypersthene, Eulite and ferrosilite are the primary pyroxenes in the mafic pyroxene series. Intermediate members (hypersthene–eulite) define the En–Fs–Hd continuum typical of basaltic systems.

Plagioclase Series

$$\Upsilon_m\ [\mathcal{Q} + \mathcal{N}]_{x+y} + [x]_p(\mathcal{Q} + \mathcal{N})]_{x+y} = \mathrm{CaAl_2Si_2O_8} + \mathrm{NaAlSi_3O_8}$$

At p= 0 p = 0 p=0, Anorthite ($CaAl_2Si_2O_8$) crystallizes; at p=1p = 1p=1, Albite ($NaAlSi_3O_8$) dominates. The An–Ab series quantifies the feldspar evolution trend in the felsic–mafic transition.

Metrical Matrix Approach

Metrical matrices were applied to model ionic substitution and cation-coupled exchanges in silicate minerals, These matrices quantify crystallographic constraints in olivine–feldspar and pyroxene–feldspar systems, providing insight into crystal–melt equilibria and compositional evolution under anhydrous conditions.

Metrical Matrix for Mafic Olivine and Feldspars;

$$[\Upsilon_1(\mathcal{Q}_2\ \mathcal{N}_2)]0_8 + \mathrm{X}_1(\mathcal{Q}_3\ \mathcal{N})0_8 = [(1,\ 0], [2,\ 0)] + [(0,\ 1], [3,\ 1)]$$

$$[\beta_2](\mathrm{Z}_0)_{\bar{o}} + \quad [\alpha_2](\mathrm{Z}_0)_{\bar{o}} \ = \quad [2,\ 0] \quad + \quad [0,\ 2]$$

$$\begin{bmatrix} Anorthite \\ Forsterite \end{bmatrix} + \begin{bmatrix} Albite \\ Fayalite \end{bmatrix} = \begin{bmatrix} Anorthoclase \\ Olivine \end{bmatrix}$$

Metrical Matrix for Mafic Pyroxene and Feldspar

$$\begin{bmatrix} Ca_1[Al_2\,Si_2]O_8 \\ [Mg_2]\,Si_2O_6 \end{bmatrix} + \begin{bmatrix} Na_1[AlSi_3]O_8 \\ [Fe_2]\,Si_2O_6 \end{bmatrix} = \begin{bmatrix} (Ca_1Na_1)Al_3\,Si_5]O_{16} \\ [MgFe]\,Si_2O_6 \end{bmatrix}$$

$$\begin{bmatrix} Anorthite \\ Enstatite \end{bmatrix} + \begin{bmatrix} Albite \\ Ferrosilite \end{bmatrix} = \begin{bmatrix} Anorthoclase \\ Pyroxene \end{bmatrix}$$

Results and Discussion

Background & Regional Geology

Describes the Jos Plateau as a high-relief Neogene–Quaternary dome in north-central Nigeria characterized by massive volcanic activity. Discusses the NNW–SSE-trending structural controls, the relationship with the Cameroon Volcanic Line (CVL), and the mineralogical assemblage of the Twin Panyam basalt (olivine, clinopyroxene, labradorite, Fe–Ti oxides).

Chemical Classification of the Twin Panyam Basaltic Rocks

The basaltic rocks of the Kerang Twin Volcanoes are classified using their major oxide compositions and these are shown in Tables 1 and 2 below. The SiO_2 contents range between 45.8–52.4 wt %, while total alkalis ($Na_2O + K_2O$) vary from 3.1–5.7 wt %, indicating a mildly alkaline character. The Fe_2O_3/MgO ratios (1.6–2.3) and $TiO_2 > 1$ wt % further suggest a transitional to alkaline affinity, typical of intraplate continental basalts. The classification aligns with the tholeiitic–alkaline basalt spectrum of Yoder and Tilley (1962) and corresponds to basaltic magmas derived from a heterogeneous upper-mantle source that experienced limited fractional crystallization prior to eruption.

Table 1. Average Chemical and mineralogical compositions of LKIC 2, LKIC 4, LKIC 5 in the Twin Panyam Basaltic Rocks.

Chemical Composition (in weight percent) [a]	
SiO_2	46
Al_2O_3	13
Fe_2O_3	12
FeO	
MgO	11
CaO	9
Na_2O	3
K_2O	2
TiO_2	2
P_2O_3	0.2
	98.9

Petrographic Characteristics

Petrographic examination of six thin sections under plane- and cross-polarized light reveals that the rocks are fine- to medium-grained porphyritic basalts composed mainly of olivine, clinopyroxene (augite–titanaugite), and plagioclase (labradorite), with opaque oxides (magnetite ± ilmenite) as accessories (Plates 1-3). Groundmass textures range from intergranular to intersertal, and vesicular forms are partially filled with secondary calcite and chlorite. Olivine phenocrysts display variable degrees of iddingsitization along grain boundaries, whereas pyroxenes exhibit well-developed cleavages and simple twinning. These textural relationships indicate rapid cooling and crystallization from mildly alkaline basaltic magma, consistent with a volcanic origin under subaerial conditions (Isah et al. 2023; Mohammed et al. 2014).

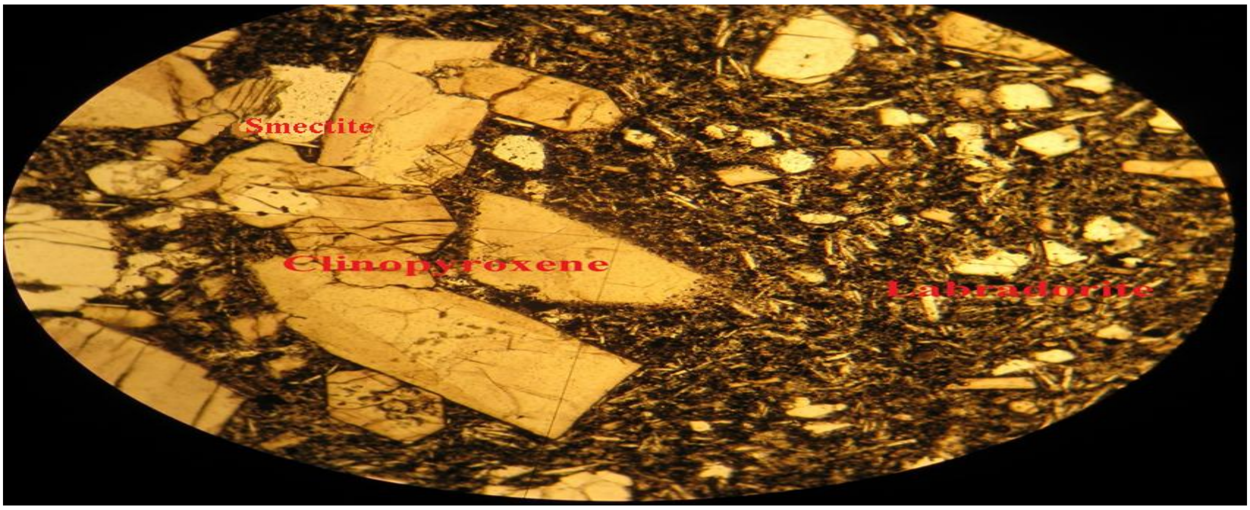

Figure 1. LKIC 2a: Photomicrograph of LKIC 2 (PPL) of the Twin Panyam Basaltic Rock rock with large broken and clotted Phenocrysts of clinopyroxenes enclosed in needle like labradorite laths (X40).

Petrogenetic Affiliation

The observed mineral assemblage (olivine + clinopyroxene + plagioclase ± Fe-Ti oxides) and the alkaline geochemical character collectively support derivation from a slightly enriched upper-mantle source, likely a lherzolitic mantle domain. Trace-element ratios such as Nb/Y > 1.0 and $Zr/TiO_2 \approx 0.01 - 0.03$ corroborate an intraplate basaltic setting, while moderate Fe enrichment suggests partial fractionation of olivine and clinopyroxene during magma ascent. This evolutionary trend aligns with a calc-alkaline to mildly alkaline series, transitional between the tholeiitic and sodic suites (Dickson & Ogbonnaya Okechukwu Ukegbu, 2024).

Table 2. Empirical Formula for the Mafic Oxides of Olivine of LKIC2, LKIC4, and LKIC5

Oxides of the mineral	MgO	FeO	SiO_2
% compositios of the Oxides	15.80	16.90	67.30
Molar mass of the Oxides	40	68	60
$\frac{\%composition}{\text{Molar mass}}$	$\frac{15.80}{40}$	$\frac{16.90}{68}$	$\frac{67.30}{60}$
Ratio of the Oxides	0.306	0.249	1.122
Divide by the smallest number	$\frac{0.395}{0.249}$	$\frac{0.211}{0.249}$	$\frac{1.122}{0.249}$
	1.6	1	4.5
	16	10	45
	$(MgO)_{16}$	$(FeO)_{10}$	$(SiO_2)_{45}$
	$Mg_{16}O_{16}$	$Fe_{10}O_{10}$	$Si_{45}O_{90}$
Empirical formula of the Oxides	$(Mg_{16}Fe_{10})\ O_{26}$		$Si_{45}O_{90}$
Chemical formula of the mineral	$(Mg_{16}Fe_{10})\ Si_{45}O_{116}$		
Mineral 1	Olivine		
Mineral 1 + SiO_2	$(Mg_{16}Fe_{10})\ Si_{46}O_{118}$		
Mineral 2	Pyroxene		

$(Mg_{16}Fe_{10})Si_{45}O_{116}$ can be converted to true value of Olivine Mineral using Zero polynomial of $Mg_{2-p}Fe_pSiO_4$

$[Mg+iFe]_5Si_5O_{20} = Mg_{10}Si_5O_{20} + i[Mg_6Fe_4]\ Si_5O_{20} + i2[Mg_4Fe_6]\ Si_5O_{20} + Fe_{10}Si_5O_{20}$, where p represents the substitution coefficient of Fe^{2+} for Mg^{2+} in the forsterite–fayalite continuum. At p = 0, pure forsterite (Mg_2SiO_4) crystallizes; at p = 2, pure fayalite (Fe_2SiO_4) forms. Computed empirical compositions from the Panyam basalts yield intermediate olivine ($Fo_{60}Fo_{40}$), corresponding to hyalosiderite–hortonolite, signifying moderate Fe enrichment and crystallization under oxygen fugacities consistent with sub-alkaline to mildly alkaline basaltic magma. This compositional spread supports fractional crystallization under decreasing temperature and moderate pressure, typical of intraplate volcanic systems (Houshmand-Manavi et al., 2025).

Empirical and Mathematical Modelling of Mineral Series

Empirical formula and classifications for Mafic Oxides of Olivine of LKIC2, LKIC4, and LKIC5 inthe Twin Panyam basaltic rock using Zero Polynomial of $(\boldsymbol{\beta}_{2-p}\alpha_p)(Z_0)_{\bar{o}}$

Mafic Olivine Series

Empirical modelling based on Achuenu et al. (2025) expresses the olivine solid-solution series. Therefore, the chemical compositions of mafic oxides of Olivine can be expressed using empirical formula as shown in Table 3 below.

Table 3. Empirical Formula for the Mafic Oxides of Olivine of LKIC2, LKIC4, and LKIC5

Oxides of the mineral	MgO	FeO	SiO_2
% composition of the Oxides	15.80	16.90	67.30
Molar mass of the Oxides	40	68	60
$\frac{\%composition}{\text{Molar mass}}$	$\frac{15.80}{40}$	$\frac{16.90}{68}$	$\frac{67.30}{60}$
Ratio of the Oxides	0.306	0.249	1.122
Divide by the smallest number	$\frac{0.395}{0.249}$	$\frac{0.211}{0.249}$	$\frac{1.122}{0.249}$
	1.6	1	4.5
	16	10	45
	$(MgO)_{16}$	$(FeO)_{10}$	$(SiO_2)_{45}$
	$Mg_{16}O_{16}$	$Fe_{10}O_{10}$	$Si_{45}O_{90}$
Empirical formula of the Oxides	$(Mg_{16}Fe_{10})\ O_{26}$		$Si_{45}O_{90}$
Chemical formula of the mineral	$(Mg_{16}Fe_{10})\ Si_{45}O_{116}$		
Mineral 1	Olivine		
Mineral 1 + SiO_2	$(Mg_{16}Fe_{10})\ Si_{46}O_{118}$		
Mineral 2	Pyroxene		

Geothermobarometric Modeling and Thermal Evolution

The temperature and pressure conditions that govern the crystallization of mineral assemblages in the Twin Panyam volcanic rocks were evaluated using classical mineral equilibria models and empirical geothermobarometric equations. These calculations are based on mineral chemistry data obtained from electron microprobe analyzes of coexisting olivine, pyroxene, and plagioclase phases.

Geothermometric Analysis using "Bowens Index -Temperature Model

Bowens Index -Temperature Model is a Geometric Arrangement of minerals in Rocks with respect to Index number of minerals as observed under microscope and Temperature of cooling of minerals as shown in Figure (1) below. It helps to give a specific name of a mineral from corresponding silicate identity, e.g., Hyalosiderite is an Olivine mineral because it has a corresponding olivine identity and it corresponds simultaneously to both Labradorite and tridynmite at the same temperature which are the geothermometers as shown in Figure 1 below, therefore if you know the index number of the mineral you observed under microscope and the corresponding temperature of formation, then you can identify the specific name of the mineral using the "Bowens Index -Temperature Model". Here are the two parameters that were used to design "Bowens Index – Temperature Model" :Index number of minerals as observed under microscope; Temperature of cooling minerals.

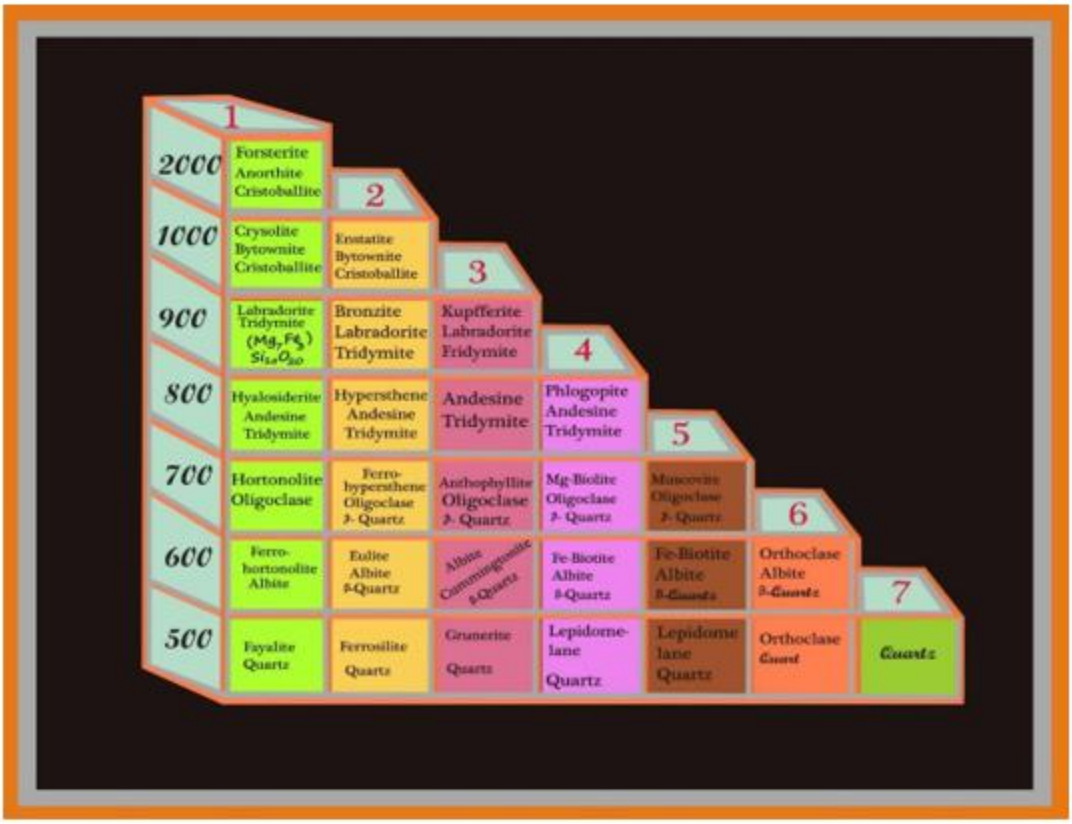

Figure 2. Bowens Index-Temperature Model.

Mineral–Melt Equilibrium and Thermodynamic Modeling

Understanding mineral–melt equilibrium provides vital constraints on the physicochemical evolution of the magma from which the Twin Panyam volcanoes crystallized. This section employs thermodynamic modeling and partition coefficient analysis to evaluate equilibrium relationships between coexisting mineral phases (olivine, pyroxene, and plagioclase) and their parental melts. Such analyses allow inferences on magma evolution, crystallization paths, and potential source characteristics.

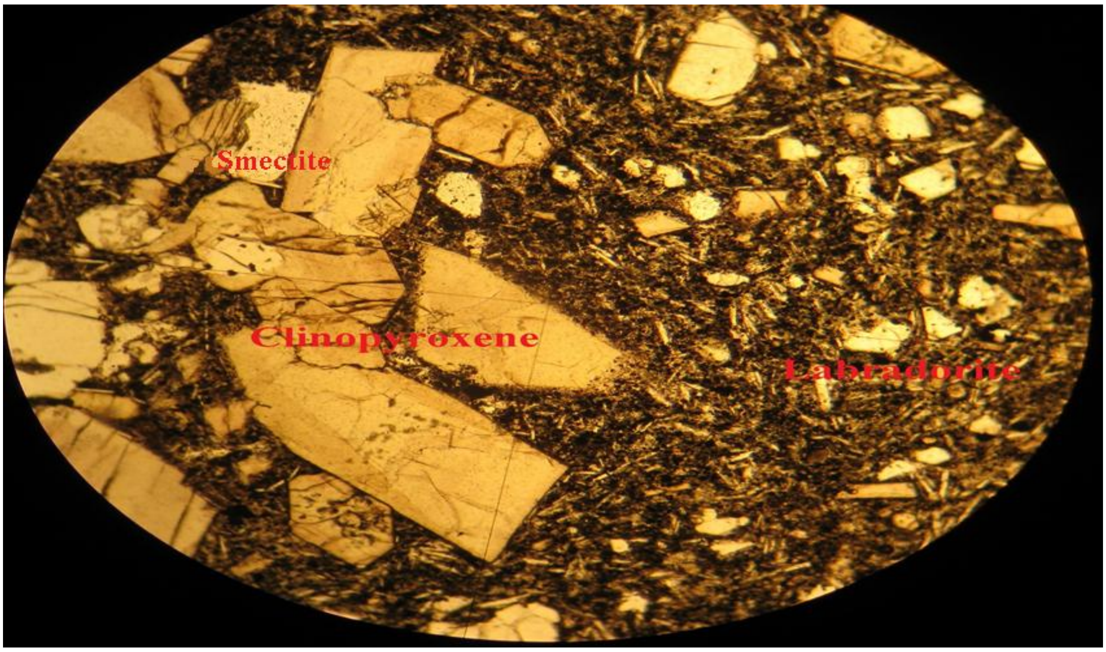

Figure 3. LKIC2 Sample from Twin Panyam Basaltic Rock, showing the Hyalosidrite, Magnesio-augite, Labrodorite and Ulvospinel at the same estimated Tridymite temperature of above 800^{0}C and pressure of 6–9 kbar

Findings From The Twin Panyam (Lkic2, Lkic4, Lkic5 Samples) Basaltic Rocks Using Matrix Method

$$\begin{bmatrix} Anorthite \\ Magnesio - augite \end{bmatrix} + \begin{bmatrix} Albite \\ Ferroaugite \end{bmatrix} = \begin{bmatrix} Labradorite \\ Augite \end{bmatrix}$$

$$\begin{bmatrix} \text{Labradorite} \\ Hyalosiderite \end{bmatrix} + \begin{bmatrix} \text{Labradorite} \\ \text{Magnesio} - \text{augite} \end{bmatrix} = [\text{Alkaline -basalt}]$$

Table 4. The average Mineralogical Compositions and Rock type from the LKIC2, LKIC4, LKIC5 Samples from Twin Panyam Basaltic Rocks at 6–9 kbar and 800^{0}C.

Minerals	Olivine	Clino-pyroxene	Feldspar	Iron ore	Silica	Others
Chemical formula	$Mg_{21}Fe_{19}(Si_2O_8)_{10}$	$[(Ca_5Fe_6Mg_{16})](Si_2O_6)_{10}$	$Ca_3Na_2(Al_4Si_{12})O_{34}$	$(Fe_6Ti)(O_8)$	SiO_2	
Mineral type	Hyalosiderite	Magnesio-augite	Bytownite	Ulvospinel	Tridymite	
Temp(^{0}C)	800-1000	800-1000	800-1000	800-1000	800-1000	
Alkali content	$Na_2O + K_2O = 5.66\%$ $Na_2O + K_2O > 3\%$					
Rock type	Alkaline Basalt, Gabbro.					

Minerals from the twin Panyam basaltic rocks as shown in Tables 9 above, are Magnesio-augite (Basic Clino-pyroxene), Hyalosiderite (Basic olivine), Plagioclase: Labradorite (Basic Plagioclase) and Ulvospinel (Iron ore) are the minerals estimated using Geothermometric and empirical approaches with their estimated Tridymite temperatures of above 800^{0}C and pressure of

6–9 kbar as shown in Bowen's Index Temperature Model (Fig. 1). Hyalosiderite, Magnesio-augite, Labradorite set in matrix, with total alkali less than ≤3% of $Na_2O + k_2O$, was use to classify the basaltic rocks of the twin Panyam volcanoes as alkaline basalt using an estimated Tridymite temperature of above 800^0C and pressure of 6–9 kbar to calculate the temperatures and pressures of formation of the twin Panyam basaltic rocks (Figs. 2 - 7).

Findings of The Twin Panyam (Ldic1, Ldic2, Ldic3) Basaltic Rock Using Matrix Method

$$\begin{bmatrix} Anorthite \\ Augite \end{bmatrix} + \begin{bmatrix} Albite \\ Ferroaugite \end{bmatrix} = \begin{bmatrix} Labradorite \\ Augite \end{bmatrix}$$

$$\begin{bmatrix} \text{Labradorite} \\ Hyalosiderite \end{bmatrix} + \begin{bmatrix} \text{Labradorite} \\ \text{Augite} \end{bmatrix} = [\text{Alkaline -basalt}]$$

Table 5. The Average Mineralogical Compositions and Rock type from LDIC1, LDIC2, LDIC3 sampes from the Twin Panyam Basaltic Rocks at 6–9 kbar and 800^0C

Minerals	Olivine	Clino-pyroxene	Feldspar	Iron ore	Silica	Others
Chemical formula	$Mg_{21}Fe_{19}(Si_2O_8)_{10}$	$[(Ca_6Fe_7Mg_7)](Si_2O_6)_{10}$	$Ca_3Na_2(Al_6Si_{14})O_{41}$	$(Fe_6Ti)(O_8)$	SiO_2	
Mineral type	Hyalosiderite	Augite	Bytownite	Ulvospinel	Quartz	
					0	21
Alkali content	$Na_2O + K_2O = 4.47\%$ $Na_2O + K_2O > 3\%$					
Rock type	Alkaline Basalt, Gabbro.					

Minerals from the LDIC1, LDIC2, LDIC3 basaltic rock as shown in Tables 10 above, are Augite (Basic Clino-pyroxene), Hyalosiderite (Basic olivine), Plagioclase: Labradorite (Basic Plagioclase) and Ulvospinel (Iron ore) are the minerals estimated using Geothermometric and empirical approaches with their estimated Tridymite temperature of above 800^0C at and pressure of 6–9 kbar as shown in Bowen`s Index Temperature Model in Figure 3 above. Hence, Hyalosiderite, Augite, Labradorite set in matrix, with total alkali content of less than 3% ($Na_2O + k_2O < 3\%$), to form an estimated basic rock in classification called alkaline basalt and its estimated Tridymite temperature of above 800^0C at and pressure of 6–9 kbar.

Discussion

Petrogenetic Context within the Jos Plateau Volcanic Province

The Twin Panyam volcanoes represent a significant component of the Cenozoic alkaline volcanic suite of the Jos Plateau, characterized by mantle-derived basaltic magmas emplaced along pre-existing structural lineaments. The integrated interpretation of mineralogy, mineral chemistry, petrographic textures, and trace-element systematics indicates that the magmas exhibit an intraplate geochemical signature and were generated by partial melting of an enriched lithospheric mantle source, with a minor but discernible contribution from the asthenosphere. The compositional characteristics of olivine (Fo_{82}–Fo_{70}) and clinopyroxene (Wo_{45}–En_{40}–Fs_{15}) phenocrysts, together with REE profiles marked by pronounced LREE enrichment and nearly flat HREE patterns, collectively suggest melting within the garnet stability field. These signatures imply magma generation at depths of approximately 80–100 km, consistent with mantle melting beneath intraplate volcanic provinces influenced by deep-seated lithospheric heterogeneities (Ward et al., 2021); (Yang et al., 2026).

Magmatic Evolution and Differentiation

The crystallization sequence inferred from petrographic observations—olivine followed by clinopyroxene, plagioclase, and late-stage Fe–Ti oxides—together with progressive Fe–Mg exchange trends in the ferromagnesian minerals, supports closed-system fractional crystallization as the principal differentiation mechanism. Geothermometric estimates of 800–1,000 °C indicate an early high-temperature stage of magma evolution, whereas barometric constraints of 6–9 kbar suggest polybaric crystallization spanning from upper-mantle to mid-crustal depths. The presence of modest negative Eu anomalies in some of the more evolved basalts further corroborates the role of plagioclase fractionation during the later stages of differentiation. These petrological and geochemical features are consistent with evolutionary trends documented in other volcanic centers of the Jos Plateau, including Kerang, Kassa, and Biu, where polybaric magma evolution and limited crustal assimilation have been recognized as key controls on magma differentiation (Hutchison et al., 2018); (Marxer et al., 2022).

Geodynamic and Structural Implications

The alignment of the Twin Panyam volcanoes along a NNW–SSE-trending fracture system underscores the strong tectonic control exerted by the West African Central Lineament (WACL), a major lithospheric weakness zone that facilitated magma ascent during Cenozoic volcanism (Alonso-Perez & Day, 2021); (Tian et al., 2023). The Neogene–Quaternary basaltic activity in central Nigeria is therefore interpreted as a manifestation of regional lithospheric reactivation following the cessation of Pan-African orogenic stabilization (Ju et al., 2022). Mantle-derived alkaline magmatism in this region appears closely linked to localized asthenospheric upwelling beneath the rejuvenated lithosphere, analogous to magmatic processes documented along the Cameroon Volcanic Line (CVL) and within segments of the East African Rift System (EARS) (Adams, 2022); (Hasegawa et al., 2025); (Djamilatou et al., 2025). Consequently, the Twin Panyam volcanic line represents a post-orogenic intraplate magmatic phase and may be viewed as the northernmost expression of CVL-type alkaline magmatic activity within the West African Rift domain (Pouclet et al., 2017); (Ayalew & Abebe, 2022).

Comparative Insights with Global Alkaline Provinces

When compared with other intraplate volcanic provinces, the geochemical characteristics of the Twin Panyam basalts—particularly their moderate alkali contents, ocean-island-basalt (OIB)–like trace element patterns, and absence of subduction-related anomalies—firmly position them within the global suite of intraplate alkaline basaltic systems, such as those of the Canary Islands, Hoggar, and Tibesti provinces (Kamaunji et al., 2026); (Wiemer et al., 2023). The mantle source heterogeneity inferred from diagnostic trace element ratios (e.g., La/Nb, Th/Nb, and Ba/La) further supports derivation from a metasomatized lithospheric mantle, likely modified by earlier subcontinental enrichment processes (Holwell et al., 2019); (Chilson-Parks et al., 2022). Such enrichment provides a plausible explanation for the trace-element variability observed among basalts across the broader Jos Plateau volcanic field (Ayalew et al., 2016); (Tortelli et al., 2026).

Conclusion

The Twin Panyam volcanoes represent mantle-derived, mildly alkaline basaltic magmatism emplaced along reactivated basement fractures associated with the West African Central Lineament (WACL); Petrographic, geochemical, and mineral chemical evidence collectively demonstrates that the basalts evolved through polybaric fractional crystallization with minimal crustal assimilation; Estimated crystallization conditions (T = 800–1,000 °C; P = 6–9 kbar) indicate magma generation and differentiation within the lithospheric mantle, specifically within the garnet lherzolite stability field; Trace-element systematics—marked by strong LREE enrichment and moderate HFSE depletion—reflect an OIB-like mantle signature, confirming a within-plate magmatic origin;; The Twin Panyam volcanic centers constitute the northern expression of Neogene–Quaternary intraplate basaltic volcanism related to mantle upwelling and lithospheric reactivation, analogous to magmatic processes along the Cameroon Volcanic Line; The integration of mineral chemistry, thermodynamic modeling, and whole-rock geochemistry provides new insights into the petrogenetic and geodynamic evolution of the Panyam volcanic line, thereby contributing to a broader understanding of Cenozoic intraplate magmatism within the West African Rift–Plateau system.

Conflicts of Interest

There were no Conflicts of Interest

Funding

The research and writing of this article were funded by personal funds.

Declaration of generative AI in scientific writing

The authors acknowledge the use of generative artificial intelligence (Grammarly tool) exclusively for language editing, grammar refinement, and improving the academic phrasing of this manuscript. The AI assistance was utilized solely to polish the text and enhance readability. The authors reviewed, edited, and verified all final content to ensure accuracy and take full responsibility for the integrity of the research.

Author Contributions

Conceptualization, methodology, validation; formal analysis, investigation; resources, data curation; original draft writing; review and editing, visualization. All authors have read and approved the final manuscript: L. I. C., A. I., & L. U. A.

References

Acosta-Nagle, A. E., Díaz-Alvarado, J., Fernández, C., Christiansen, R., D'Eramo, F. J., Pinotti, L. P., López, J. P., & Bellos, L. I. (2025). Studying the kinematics of magma emplacement in fabric-weak, epizonal plutons: The example of the Sauce Guacho and Santa Rosa plutons, eastern Sierras Pampeanas, Argentina. *Journal of Structural Geology*, *190*, 105294. https://doi.org/10.1016/j.jsg.2024.105294

Adams, A. (2022). Insights Into the Source of Magmatic Hot-Lines: Forty Years of Geophysical Studies of the Cameroon Volcanic Line. *Frontiers in Earth Science*, *10*, 838993. https://doi.org/10.3389/feart.2022.838993

Alonso-Perez, R., & Day, J. M. D. (2021). Rare Earth Element and Incompatible Trace Element Abundances in Emeralds Reveal Their Formation Environments. *Minerals*, *11*(5), 513. https://doi.org/10.3390/min11050513

Ayalew, D., & Abebe, B. (2022). Mineralogy of Peralkaline Silicic Volcanics: Information from Kone Volcano, Ethiopian Rift Valley. In M. René (Ed.), *Mineralogy*. IntechOpen. https://doi.org/10.5772/intechopen.102677

Ayalew, D., Jung, S., Romer, R. L., Kersten, F., Pfänder, J. A., & Garbe-Schönberg, D. (2016). Petrogenesis and origin of modern Ethiopian rift basalts: Constraints from isotope and trace element geochemistry. *Lithos*, *258–259*, 1–14. https://doi.org/10.1016/j.lithos.2016.04.001

Benamrane, M., Németh, K., Jadid, M., & Talbi, E. H. (2022). Geomorphological Classification of Monogenetic Volcanoes and Its Implication to Tectonic Stress Orientation in the Middle Atlas Volcanic Field (Morocco). *Land*, *11*(11), 1893. https://doi.org/10.3390/land11111893

Cedric Bernard, L., & Uriah Alexander, L. (2022). Hydrogeochemistry of the Pidong Crater Lake, Jos Plateau Volcanic Province, Nigeria: Constraints on Chemical Elements Sources. In A. Paone & S.-H. Yun (Eds.), *Progress in Volcanology*. IntechOpen. https://doi.org/10.5772/intechopen.99720

Chilson-Parks, B. H., Calabozo, F. M., Saal, A. E., Wang, Z., Mallick, S., Petrinovic, I. A., & Frey, F. A. (2022). The Signature of Metasomatized Subcontinental Lithospheric Mantle in the Basaltic Magmatism of the Payenia Volcanic Province, Argentina. *Geochemistry, Geophysics, Geosystems*, *23*(1), e2021GC010071. https://doi.org/10.1029/2021GC010071

Dickson, S. M. & Ogbonnaya Okechukwu Ukegbu. (2024). IoT-Enabled Smart Agriculture: A Pathway to Nigeria's Economic Recovery and Sustainable. *Radinka Journal Of Science And Systematic Literature Review*, *2*(2), 313–318. https://doi.org/10.56778/rjslr.v2i2.252

Djamilatou, D. H., Gountié Dedzo, M., Lenhardt, N., Tsozué, D., Asobo Nkengmatia, E. A., & Klamadji Ngarena, M. (2025). Crystallisation and petrogenesis of Cenozoic alkaline basaltic lavas on the Kapsiki Plateau (Moukoulvi, Far-North Cameroon): Unveiling the mantle's heterogeneity and HIMU signature. *Solid Earth Sciences*, *10*(2), 100231. https://doi.org/10.1016/j.sesci.2025.100231

Hasegawa, T., Aka, F. T., Iwamori, H., Watanabe, S., Asaah, A. N. E., & Linus, N. (2025). Did magmatism of the Central Atlantic Magmatic Province (CAMP) extend to the proto-Cameroon Line in the Gulf of Guinea (West/Central Africa)? *Earth, Planets and Space*, *77*(1), 157. https://doi.org/10.1186/s40623-025-02275-w

Hategekimana, F., Naik, S. P., & Kim, Y.-S. (2024). Morphological analysis of volcanic cones and its implication to Quaternary tectonics of the Jeju Island (South Korea). *Quaternary Science Advances*, *13*, 100169. https://doi.org/10.1016/j.qsa.2024.100169

Heineke, C., Niedermann, S., Hetzel, R., & Akal, C. (2016). Surface exposure dating of Holocene basalt flows and cinder cones in the Kula volcanic field (Western Turkey) using cosmogenic 3He and 10Be. *Quaternary Geochronology*, *34*, 81–91. https://doi.org/10.1016/j.quageo.2016.04.004

Holwell, D. A., Fiorentini, M., McDonald, I., Lu, Y., Giuliani, A., Smith, D. J., Keith, M., & Locmelis, M. (2019). A metasomatized lithospheric mantle control on the metallogenic signature of post-subduction magmatism. *Nature Communications*, *10*(1), 3511. https://doi.org/10.1038/s41467-019-11065-4

Houshmand-Manavi, S., Rezaei-Kahkhaei, M., Klötzli, U., & Ghasemi, H. (2025). Crystallization Conditions of Basaltic Lavas Based on Clinopyroxene and Olivine Phenocryst Petrology: A Case Study from the Neogene Lavarab Alkaline Basaltic Lavas (LABL), Eastern Iran. *Minerals*, *15*(9), 915. https://doi.org/10.3390/min15090915

Hutchison, W., Mather, T. A., Pyle, D. M., Boyce, A. J., Gleeson, M. L. M., Yirgu, G., Blundy, J. D., Ferguson, D. J., Vye-Brown, C., Millar, I. L., Sims, K. W. W., & Finch, A. A. (2018). The evolution of magma during continental rifting: New constraints from the isotopic and trace element signatures of silicic magmas from Ethiopian volcanoes. *Earth and Planetary Science Letters*, *489*, 203–218. https://doi.org/10.1016/j.epsl.2018.02.027

Issatayeva, F., Abetov, A., Umirova, G., Abdullina, A., Mustafin, Z., & Karpenko, O. (2025). The Roles of Transcrustal Magma- and Fluid-Conducting Faults in the Formation of Mineral Deposits. *Geosciences*, *15*(6), 190. https://doi.org/10.3390/geosciences15060190

Jimenez, M., Holford, S., King, R., & Bunch, M. (2025). Structural controls on post-rift magmatism in the Ceduna Sub-basin, Great Australian Bight. *Australian Journal of Earth Sciences*, *72*(7), 853–871. https://doi.org/10.1080/08120099.2025.2542223

Ju, Y., Wang, G., Li, S., Sun, Y., Suo, Y., Somerville, I., Li, W., He, B., Zheng, M., & Yu, K. (2022). Geodynamic mechanism and classification of basins in the Earth system. *Gondwana Research*, *102*, 200–228. https://doi.org/10.1016/j.gr.2020.08.017

Kamaunji, V. D., Ahmed, H. A., Wang, L.-X., Sanislav, I. V., Girei, M. B., Zhu, Y.-X., Liang, X., Chen, X., & Sami, M. (2026). Progressive mantle melting and crust–mantle–fluid hybridization in fluorite-bearing Sn–Nb ± Mo-rich alkaline granites of the Jos Plateau, central Nigeria. *Ore Geology Reviews*, *195*, 107405. https://doi.org/10.1016/j.oregeorev.2026.107405

Kang, D., Woo, J., & Kil, Y. (2025). Volcanic facies analysis of the Quaternary Hantangang Basalt, Korea: Implications for lava flow field architecture and emplacement history. *Bulletin of Volcanology*, *87*(12), 108. https://doi.org/10.1007/s00445-025-01902-4

Lima, A. T., & Ottosen, L. (2021). Recovering rare earth elements from contaminated soils: Critical overview of current remediation technologies. *Chemosphere*, *265*, 129163. https://doi.org/10.1016/j.chemosphere.2020.129163

Martínez-Casado, R., Todorović, M., Mallia, G., Harrison, N. M., & Pérez, R. (2019). First Principles Calculations on the Stoichiometric and Defective (101) Anatase Surface and Upon Hydrogen and H2Pc Adsorption: The Influence of Electronic Exchange and Correlation and of Basis Set Approximations. *Frontiers in Chemistry*, *7*, 220. https://doi.org/10.3389/fchem.2019.00220

Marxer, F., Ulmer, P., & Müntener, O. (2022). Polybaric fractional crystallisation of arc magmas: An experimental study simulating trans-crustal magmatic systems. *Contributions to Mineralogy and Petrology*, *177*(1), 3. https://doi.org/10.1007/s00410-021-01856-8

Neave, D. A., Stewart, A. G., Hartley, M. E., & McCammon, C. (2024). Re-evaluating stoichiometric estimates of iron valence in magmatic clinopyroxene crystals. *Contributions to Mineralogy and Petrology*, *179*(1), 5. https://doi.org/10.1007/s00410-023-02080-2

Németh, K., & Kósik, S. (2020). The role of hydrovolcanism in the formation of the Cenozoic monogenetic volcanic fields of Zealandia. *New Zealand Journal of Geology and Geophysics*, *63*(4), 402–427. https://doi.org/10.1080/00288306.2020.1770304

Pompa-Mera, V., Rodríguez-Elizarrarás, S. R., & Morales-Barrera, W. V. (2026). Arc-related subalkaline magmas at the Los Tuxtlas volcanic complex and its relation to the tectonic evolution in southern México. *International Geology Review*, *68*(5), 507–527. https://doi.org/10.1080/00206814.2025.2587304

Pouclet, A., El Hadi, H., Bardintzeff, J.-M., Benharref, M., & Fekkak, A. (2017). Devonian to Early Carboniferous magmatic alkaline activity in the Tafilalt Province, Eastearn Morocco: An Eovariscan episode in the Gondwana margin, north of the West African Craton. *Journal of African Earth Sciences*, *129*, 814–841. https://doi.org/10.1016/j.jafrearsci.2017.01.030

Principe, C., Giordano, D., Paolillo, A., Arrighi, S., Brocchini, D., & La Felice, S. (2024). Structural Control at Monte Somma and Vesuvio during the Last 5600 Years through Time and Space Distribution of Volcanic Vents. *Geosciences*, *14*(4), 91. https://doi.org/10.3390/geosciences14040091

Rojas, M. C., Mantegazza, M., Bishop, J. L., & Spagnuolo, M. G. (2026). Geomorphology and Mineralogy of Belén Crater in Iani Chaos (Mars) Point to Hydrothermal Activity. *The Planetary Science Journal*, *7*(5), 130. https://doi.org/10.3847/PSJ/ae5dcb

Scivetti, I., & Teobaldi, G. (2023). ALC_EQCM: Automated stoichiometric resolution in electrochemistry through Density Functional Theory aided, Electrochemical Quartz Crystal Microbalance. *Computational Materials Science*, *218*, 111968. https://doi.org/10.1016/j.commatsci.2022.111968

Szakács, A., & Kovacs, M. (2022). Volcanic Landforms and Landscapes of the East Carpathians (Romania) and Their Geoheritage Values. *Land*, *11*(7), 1064. https://doi.org/10.3390/land11071064

Tian, Y., Zeng, L., Shen, Y., Yan, L., Zhao, L., Xu, Q., Li, G., & Di, Y. (2023). Melting a melt-metasomatized subcontinental lithospheric mantle: Evidence from Oligocene lamproites within the Gangdese batholith, southern Tibet. *Lithos*, *448–449*, 107163. https://doi.org/10.1016/j.lithos.2023.107163

Tomasi, I., Tonello, M., Massironi, M., Tesson, P.-A., Sauro, F., Meyzen, C. M., Martìnez-Frìas, J., & Mederos, E. M. (2023). Geology of Lanzarote's northern region (Canary Island, Spain). *Journal of Maps*, *19*(1), 2187717. https://doi.org/10.1080/17445647.2023.2187717

Tortelli, G., Crescenzi, P., Pagli, C., Gioncada, A., Keir, D., & Pagli, L. (2026). Cluster analysis reveals increasing plume-like magmatism during progressive rifting in Afar (Ethiopia). *Scientific Reports*, *16*(1), 6843. https://doi.org/10.1038/s41598-026-35961-0

Udoinyang, N. (2025). Accessing National Demand-Side Climate Change Mitigation Plan and Socio-Economic Impact in Nigeria. *Radinka Journal Of Science And Systematic Literature Review*, *3*(2), 701–709. https://doi.org/10.56778/rjslr.v3i2.563

Verolino, A., Jenkins, S. F., Sieh, K., Herrin, J. S., Schonwalder-Angel, D., Sihavong, V., & Oh, J. H. (2022). Assessing volcanic hazard and exposure to lava flows at remote volcanic fields: A case study from the Bolaven Volcanic Field, Laos. *Journal of Applied Volcanology*, *11*(1), 6. https://doi.org/10.1186/s13617-022-00116-z

Ward, J. F., Rosenbaum, G., Ubide, T., Wu, J., Caulfield, J. T., Sandiford, M., & Gürer, D. (2021). Geophysical and geochemical constraints on the origin of Holocene intraplate volcanism in East Asia. *Earth-Science Reviews*, *218*, 103624. https://doi.org/10.1016/j.earscirev.2021.103624

Wiemer, D., Hagemann, S. G., Hayward, N., Begg, G. C., Hronsky, J., Thébaud, N., Kemp, A. I. S., & Villanes, C. (2023). Cryptic trans-lithospheric fault systems at the western margin of South America: Implications for the formation and localization of gold-rich deposit superclusters. *Frontiers in Earth Science*, *11*, 1159430. https://doi.org/10.3389/feart.2023.1159430

Yang, J., Faccenda, M., Meyzen, C. M., Marzoli, A., & Zhao, L. (2026). Subduction legacies in the mantle transition zone modulate intraplate oceanic volcanism. *Nature Communications*, *17*(1), 6566. https://doi.org/10.1038/s41467-026-73403-7